obtained, for example, $0.4 < U/U^* < 0.9$; and, an LCO with two frequencies results in four points, etc. A large number of points at some velocities indicates aperiodic or possibly chaotic motion, for example, $0.27 < U/U^* < 0.33$. The finite difference results give only one stable solution for each given set of initial conditions and velocity, whereas the describing function method produces all possible stable or unstable solution regardless of the initial conditions.

As shown in Fig. 2, the system has three stable LCOs and one stable equilibrium solution below the linear flutter speed. In addition to the LCO solutions, the finite difference results show nonperiodic type motions for some airspeeds, most notably $0.27 < U/U^* < 0.33$. For a speed range $U/U^* < 0.32$, Fig. 2 indicates the possibility of two stable period-one LCOs. These oscillations are analyzed via power spectral density. Power spectra obtained for the two LCOs at each speed suggest that the frequency ratio of the two oscillations is most probably irrational. This indicates the possibility of quasi-periodic oscillations, which is a precursor to the quasi-periodic route leading to chaos.

For the given set of airfoil parameters and $U/U^* = 0.3$, phase-plane plots suggest nonperiodic oscillations in all pitch, plunge, and aileron motions. Figure 3 shows power spectral densities and Poincaré sections of both the pitch and aileron motions at $U/U^* = 0.3$. The broadband frequency spectrum (Fig. 3b) and fractal-like pattern in the Poincaré map (Fig. 3d) are strong indicators of chaotic motion for the aileron motion. For the pitch motion, however, the frequency spectrum is less broadband, and it shows broadening of two frequency spikes, possibly with an irrational frequency ratio (Figs. 3a). Also, the Poincaré map of the pitch motion is nearly a closed curve (Fig. 3c). These are characteristics of either a quasi-periodic oscillation or very mild chaos obtained through the quasi-periodic route. To classify the pitch motion more precisely, Lyapunov exponents should be calculated. The difference in dynamics of the pitch and aileron motion might be explained by the weak elastic coupling between the structural modes and the aileron deflection β [that is, $r_\beta = 0.002$ and $x_\beta = 0.002$; see Eqs. (1–3)]. Based on the preceding analysis and other frequency responses not presented here, it can be concluded that there is a quasi-periodic route to chaos for this system. This clarifies the airfoil's behavior below the flutter speed, which is useful for preventing nonlinear flutter. More results and analysis of the system behavior are presented in Ref 7.

Conclusions

To properly study the three-DOF airfoil's nonlinear dynamics, aerodynamic forces for arbitrary motions of the three-DOF airfoil are derived from Theodorsen's equations by means of a Fourier analysis. Behavior of the airfoil-aileron combination is then studied taking into account a freeplay nonlinearity in the aileron hinge moment. Bifurcation analysis of the system indicates various LCO solutions for velocities well below the linear flutter boundary. For some range of airspeed, there exists two LCOs with irrational frequency ratios giving rise to quasi-periodic oscillations. Depending on the initial conditions and airspeed, quasi-periodic and chaotic oscillations are also observed for the aileron motion. Thus, these results show that proper analysis of nonlinearities will lead to a better explanation of classes of aeroelastic responses.

References

[1]Woolston, D. S., Runyan, H. L., and Andrews, R. E., "An Investigation of Effects of Certain Types of Structural Nonlinearities on Wing and Control Surface Flutter," *Journal of the Aeronautical Sciences*, Vol. 24, Jan. 1957, pp. 57–63.

[2]Brietbach, E., "Effects of Structural Nonlinearities on Aircraft Vibration and Flutter," 45th Structures and Materials AGARD Panel Meeting, AGARD Rept. 665, 1977.

[3]McIntosh, S. C., Reed, R. E., and Rodden, W. P., "Experimental and Theoretical Study of Nonlinear Flutter," *Journal of Aircraft*, Vol. 18, No. 12, 1981, pp. 1057–1063.

[4]Tang, D. M., and Dowell, E. H., "Flutter and Stall Response of a Helicopter Blade with Structural Nonlinearity," *Journal of Aircraft*, Vol. 29, No. 5, 1992, pp. 953–960.

[5]Price, S. J., Alighanbari, H., and Lee, B. H. K., "The Aeroelastic Response of a Two Dimensional Airfoil with Bilinear and Cubic Structural Nonlinearities," *Journal of Fluids and Structures*, Vol. 9, No. 2, 1995, pp. 175–193.

[6]Kholodar, D. B., Denis, B., and Dowell, E. H., "Behavior of Airfoil with Control Surface Freeplay for Nonzero Angle of Attack," *AIAA Journal*, Vol. 37, No. 5, 1999, pp. 651–653.

[7]Alighanbari, H., "Aeroelastic Response of an Airfoil-Aileron Combination with Structural Nonlinearities," *Proceedings of Third International Conference on Nonlinear Problems in Aviation*, 2000, pp. 21–30.

Camber Effects on the Near Wake of Oscillating Airfoils

Jo Won Chang*
Hankuk Aviation University,
Kyunggi 412-791, Republic of Korea
and
Yong Hyun Yoon†
Korea Air Force Academy,
Chung-buk 363-849, Republic of Korea

Nomenclature

C	=	airfoil chord
f	=	frequency of oscillation
K	=	reduced frequency, $K = \pi f C/U_\infty$
k_1, k_2	=	yaw factor
Re	=	Reynolds number
t	=	time
U_∞	=	freestream velocity
u	=	velocity component
u'	=	turbulent velocity fluctuation
X, Y	=	streamwise, normal coordinates
α	=	instantaneous angle of attack
α_0	=	mean incidence angle
α_1	=	oscillation amplitude

Introduction

THE study of the near-wake characteristics of an oscillating airfoil has significant scientific and engineering applications. The near flow behind a propeller and the near wake of a helicopter blade are perturbed by unsteady incoming flows. Both the mean velocity defect and the turbulence properties of the wakes play a significant role in the noise generation, inefficiency, and performance of the subsequence devices (for example, propeller, rotor blades, etc). Hence accurate prediction of the near-wake properties is necessary in the design of efficient airfoils.

Most of the previous research efforts in this area are directed to the phenomenon of the flow structure over the streamlined symmetric airfoils. Hah and Lakshminarayana[1] have studied the mean velocity and turbulence structure in the near wake of a symmetric airfoil (NACA 0012) experimentally and numerically. The results showed the complex nature of the near wake and its asymmetrical phenomena. Park et al.[2] investigated the characteristics of the near wakes behind a NACA 0012 airfoil at a given combination of mean

Received 25 July 2001; presented as Paper 2002-0116 at the AIAA 40th Aerospace Sciences Meeting, Reno, NV, 14–17 January 2002; revision received 6 March 2002; accepted for publication 11 March 2002.

*Assistant Professor, Department of Aeronautical Science and Flight Operation, 200-1, Hwajun-Dong, Dukyang-Gu, Koyang City. Member AIAA.

†Associate Professor, Department of Aerospace Engineering. Member AIAA.

incidence and amplitude of oscillation. The resulting wakes showed that the ensemble-averaged mean velocity and turbulence intensity profiles were considerably different from one another even when the instantaneous angles of attack were the same. Many researchers[3,4] have already revealed that the characteristics of the near wake were highly influenced by the amplitude of oscillation and freestream velocity. Attention has been rarely given to measurements of the camber effects in near wake of oscillating airfoils. The camber effect can be considered as an important parameter because the cambered airfoil has better aerodynamic characteristics[5] than the symmetrical airfoil in practice. The primary purpose of present study is to investigate the camber effects in the near-wake region of an oscillating asymmetric airfoil (NACA 4412) by taking a symmetric airfoil (NACA 0012) as a reference airfoil.

Experimental Setup and Procedure

The tests are carried out in a closed-circuit wind tunnel with a square cross section of 0.9×0.9 m and the test section length of 2.1 m. The chord and the aspect ratio of both NACA 0012 (noncambered symmetrical airfoil) and NACA 4412 airfoil (cambered airfoil) models are 0.25 and 3.4 m, respectively. Measurements are made at a freestream velocity of 12.4 m/s. The corresponding Re, based on the chord length, is 1.9×10^5, and the reduced frequency of the present work is 0.1. Under these test conditions the freestream turbulence intensity is less than 0.3%. Pitching oscillation about the $\frac{1}{4}$-chord axis is provided by a crank-connecting rod mechanism, driven by a variable-speed ac motor. The instantaneous angle of attack of the model can be expressed as varied according to $\alpha = \alpha_0 + \alpha_1 \sin 2\pi ft$, where α_0 and α_1 are set at 0 and 6 deg, respectively. Thus instantaneous angle of attack varies from -6 to $+6$ deg. Limited oscillation is produced at a small variation of instantaneous angle of attack to prevent a reverse flow because the hot-wire anemometer is unable to measure the reverse flow. Dantec's StreamLine System for the hot-wire anemometer, MetraByte's DAS1601 and sampling and hold unit (SSH-4A) are used for this measurements. The X-type hot-film probe (55R51) is mounted on a support in the center of the airfoil model span. The wake profiles are measured at four downstream stations; $X/C = 0.03, 0.08, 0.15, 0.5$. The intervals of measurement position are 2 mm in the region of wake center. One-hundred-twenty samples of velocity data, distributed evenly over one period of oscillation, are taken at a given probe position with the sampling frequency of 0.192 kHz. For each phase angle 300 ensembles are used for averaging.

The use of an X-type hot-film probe for velocity measurement involved the sensitivity problem with flow angularity. Typical values of sensitivity coefficients k_1, k_2 are 0.28 and 0.32, respectively. The velocity measurement uncertainties in the streamwise velocities are about $\pm 2.0\%$ at 20:1 odds. The temperature variations during the run time are within ± 1.5°C. The compensation of hot-film output for the change of fluid temperature is done according to Kanevce and Oka's expression.[6]

Results and Discussion

The measurement of the mean velocity and its fluctuation for the unsteady case is carried out using an X-type hot-film probe at four downstream stations. The term "upstroke motion" means the situation when the nose of the airfoil is moving upward and the term "downstroke motion" when the nose is moving downward. Thus, the

Table 1 Airfoil motion classification

Case	Phase angle	Remarks
1	0 deg $< 2\pi ft \leq 90$ deg	Upstroke motion at positive angle of attack
2	90 deg $< 2\pi ft \leq 180$ deg	Downstroke motion at positive angle of attack
3	180 deg $< 2\pi ft \leq 270$ deg	Downstroke motion at negative angle of attack
4	270 deg $< 2\pi ft \leq 360$ deg	Upstroke motion at negative angle of attack

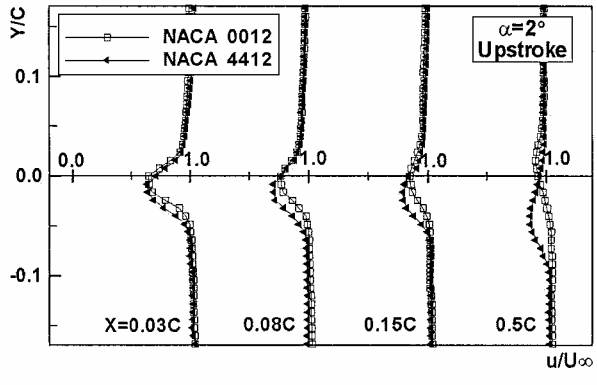

Case 1: upstroke motion at 2 deg

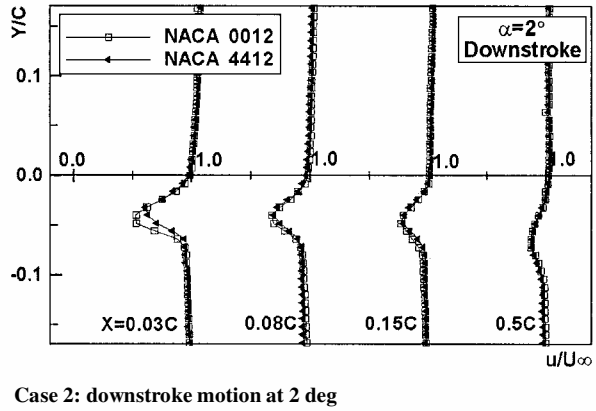

Case 2: downstroke motion at 2 deg

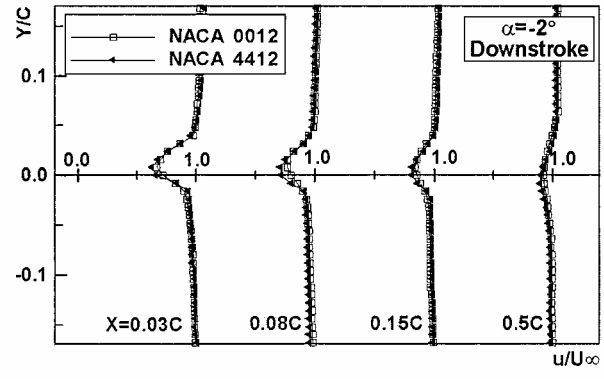

Case 3: downstroke motion at − 2 deg

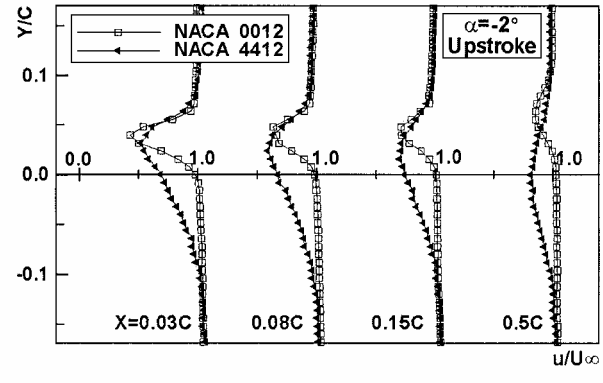

Case 4: upstroke motion at − 2 deg

Fig. 1 Streamwise velocity profiles (u/U_∞).

airfoil motion is classified into the following four cases as shown at Table 1.

The profiles of the normalized streamwise velocity component (u/U_∞) at $\alpha = \pm 2$ deg are presented in Fig. 1. Although the instantaneous angle of attack is the same for both case 1 and 2, the wake locations are different from each other. We can see that the velocity gradient of NACA 0012 airfoil at downstream stations during the downstroke motion (case 2) is steeper than that in the upstroke motion (case 1). These indicate that the velocity signal sensed at downstream stations reflects the data originated at an earlier phase angle. Thus, the true instantaneous angle of attack for the data during downstroke motion is higher than that during upstroke motion. The motions of cases 1 and 3, cases 2 and 4 are symmetric motions about X axis; hence, the velocity profile of symmetric NACA0012 airfoil is symmetric about X axis as shown at Fig. 1. We conjecture that the flow on leeward surface during the upstroke motion (case 1) and during downstroke motion (case 3) remains attached to the airfoil resulting in a wake that is less turbulent as in Ref. 7. The velocity profile shown at case 1 or 3 indicates that the wake thickness and behavior of two airfoils are similar. The camber effect cannot be found explicitly in downstroke motions as shown in the case 3. The motion of lower surface during downstroke motion at $-\alpha$ is identical with the motion of upper surface during upstroke motion at $+\alpha$. In these cases the leeward surfaces result in a thinner wake; hence, the velocity profiles are similar to each other in present measurement. The upper surface shape of NACA 4412 airfoil has a convex shape, similar to surface shape of NACA 0012 airfoil, but the lower surface shape of NACA 4412 airfoil is very different from that of NACA 0012 airfoil. We thus conjecture that a small difference in the velocity profiles is noticed for different shapes of the airfoils as a result of the flow attachment to the leeward surface during the upstroke and downstroke motions.

The velocity profiles in case 2 indicate that the wake thickness of two airfoils is similar. The degree of flow disturbance is much less than that of other studies[8] because of small oscillation amplitude and instantaneous angle of attack. Although upper surfaces of two airfoils undergo downstroke motion, the widths of velocity profiles are similar when upper surface shapes of NACA 4412 airfoil are similar to those of NACA 0012 airfoil. This reflects that very similar wake thickness and the behavior of two airfoils are caused by the similar convex shapes of upper surfaces of NACA 0012 and NACA 4412 airfoil during the downstroke motion at $+\alpha$. The airfoil section of NACA 4412 is not symmetric, whereas the motions in cases 1 and 3 are symmetric about the X axis. In these cases the leeward surfaces undergo motion that results in the flow attachment. Cases 1 and 3 of NACA 4412 airfoil are similar to each other in wake thickness and behavior.

The big difference of near-wake characteristics of two airfoils is noticed in the wake region for the case of upstroke motion at $\alpha = -2$ deg. The streamwise velocity component of the NACA 4412 airfoil in the wake region of lower surface is considerably large. The motion of lower surface during upstroke motion at $-\alpha$ is identical with the motion of upper surface during downstroke motion at $+\alpha$. Furthermore the lower surface geometry of NACA 4412 airfoil shows different surface shape (similar to flat plate) compared with the upper surface shape of two airfoils. We thus conjecture that the difference in velocity deficits of two airfoils is caused by both the different lower surface shape and the motion of the lower surface that results in the flow disturbance.

The turbulence intensity (T.I.) profiles at $\alpha = \pm 2$ deg, corresponding to the streamwise velocity profiles of Fig. 1, are shown in Fig. 2. The profiles of cases 1 and 3 and cases 2 and 4 indicate that the turbulence intensity profiles of NACA 0012 airfoil show symmetric profiles about the X axis, respectively, as a result of the symmetry of motion and airfoil shape. The profiles of cases 1 and 3 indicate that the turbulence intensity profiles of NACA 4412 airfoil show nearly symmetric profiles about the X axis. We can see that the turbulence intensity profiles are similar to each other as shown at cases 1 and 3. The upper shape of NACA 4412 airfoil has a convex shape, similar to NACA 0012 airfoil shape, but the lower shape of NACA 4412

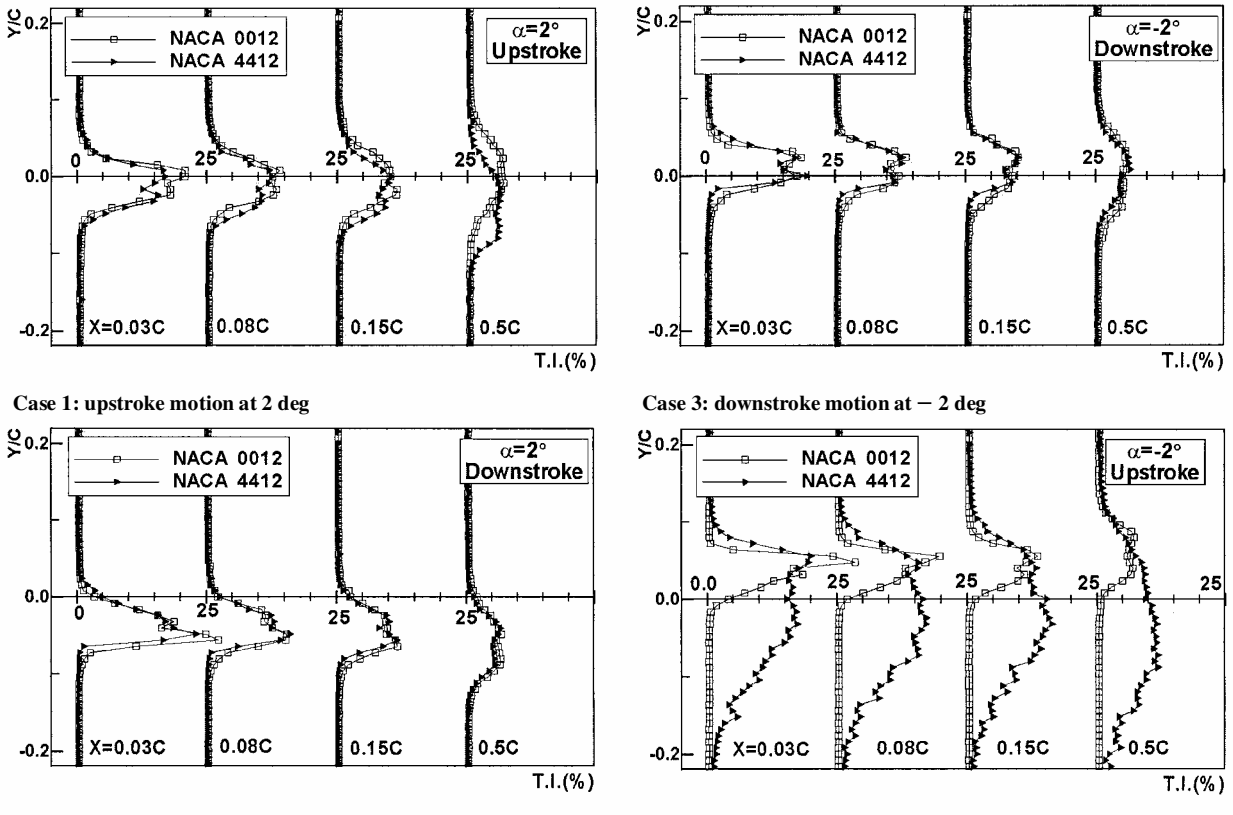

Case 1: upstroke motion at 2 deg

Case 3: downstroke motion at − 2 deg

Case 2: downstroke motion at 2 deg

Case 4: upstroke motion at − 2 deg

Fig. 2 Turbulence intensity profiles.

airfoil is very different from that of NACA 0012 airfoil. In case 3 we can see that the lower surface motion of NACA 4412 is identical with the upper surface motion as in case 1. Furthermore case 2 indicates that the turbulence intensity profiles of NACA 4412 airfoil are similar to those of NACA 0012 airfoil. Although leeward surfaces of two airfoils undergo downstroke motion, the turbulence intensity profiles have very small difference when lower surface shapes of airfoils are different. This reflects that very similar wake thickness and behavior of two airfoils is caused by the upward motion of the different lower surface shapes of NACA 0012 and NACA 4412. We thus conjecture that a small difference in the turbulence intensity profiles is noticed for different shapes of the airfoils as a result of the flow attachment to the leeward surface.

The significant difference of turbulence intensity profiles of two airfoils is shown in the wake region for the case of upstroke motion at $\alpha = -2$ deg (case 4). It is observed that the width of turbulence intensity is small for the NACA 0012 airfoil, whereas for NACA 4412 airfoil the width of turbulence intensity is much larger. When lower surface motion of NACA 4412 airfoil is identical with upper surface motion during the downstroke motion at $+\alpha$, the turbulence intensity in the wake region of lower surface is much larger than the other cases. This signifies that the flow is highly disturbed, so that the flow becomes very diffusive when the airfoil pitches up at a negative angle of attack. The difference in turbulence intensity of two airfoils is caused by both the different shape and the motion direction of lower surface.

Conclusions

Phase-averaged mean velocity and its fluctuations in the near wake of oscillating airfoils are presented. The near-wake characteristics of a NACA 0012 airfoil at $\pm\alpha$ show symmetric profiles about the X axis as a result of the symmetry of motion and airfoil shape. The velocity profiles and the turbulent intensity profiles of a NACA 4412 airfoil have small difference with those of a NACA 0012 airfoil except upstroke motion case at a negative angle of attack. These are attributable to either similar upper shape or the motion direction of the leeward surface, which result in the flow attachment to the surface. On the other hand, the significant difference of near-wake characteristics between NACA 0012 and NACA 4412 airfoil is observed in the case of upstroke motion at negative angle of attack. It is found that the streamwise velocity and turbulence intensity of the NACA 4412 airfoil in the wake region of lower surface are considerably large. These differences in streamwise velocity and turbulence intensity of two airfoils are caused by both the different lower shape and the motion direction.

References

[1]Hah, C., and Lakshminarayana, B., "Measurement and Prediction of Mean Velocity and Turbulence Structure in the Near Wake of an Airfoil," *Journal of Fluid Mechanics*, Vol. 115, 1982, pp. 251–282.

[2]Park, S. O., Kim, J. S., and Lee, B. I., "Hot-Wire Measurements of Near Wakes Behind an Oscillating Airfoil," *AIAA Journal*, Vol. 28, No. 1, 1990, pp. 22–28.

[3]Ho, C. M., and Chen, S. H., "Unsteady Wake of a Plunging Airfoil," *AIAA Journal*, Vol. 19, No. 11, 1981, pp. 1492–1494.

[4]Koochesfahani, M. M., "Vortical Patterns in the Wake of an Oscillating Airfoil," *AIAA Journal*, Vol. 27, No. 9, 1989, pp. 1200–1205.

[5]Liiva, J., "Unsteady Aerodynamic and Stall Effects on Helicopter Rotor Blade Airfoil Sections," *Journal of Aircraft*, Vol. 6, No. 1, 1969, pp. 46–51.

[6]Kanevce, G., and Oka, S., "Correcting Hot-wire Readings for Influence of Fluid Temperature Variations," *DISA Information*, No. 15, Oct. 1993, pp. 21–24.

[7]Chang, J. W., and Park, S. O., "A Visualization Study of Tip Vortex Roll-up of an Oscillating Wing," *Journal of Flow Visualization and Image Processing*, Vol. 6, No. 1, 1999, pp. 79–87.

[8]Chang, J. W., and Park, S. O., "Measurements in the Tip Vortex Roll-up Region of an Oscillating Wing," *AIAA Journal*, Vol. 38, No. 6, 2000, pp. 1092–1095.

Side Force on an Ogive Cylinder: Effects of Surface Roughness

S. C. Luo* and K. B. Lua†
National University of Singapore, Singapore 119260, Republic of Singapore
and
E. K. R. Goh‡
DSO National Laboratories, Singapore 118230, Republic of Singapore

Nomenclature

A	=	axial distance from model nose tip
Cy	=	side force coefficient, $Fy/(0.5\rho U_\infty^2 S)$
$Cy(A)$	=	local side force coefficient, local side force/$(0.5\rho U_\infty^2\ D \sin^2\alpha)$
D	=	cylinder diameter
d_{particle}	=	average diameter of aluminum oxide particles
Fy	=	side force
I	=	turbulence intensity
P	=	pressure on model surface
P_∞	=	freestream static pressure
Re_D	=	Reynolds number, $U_\infty D/\nu$
S	=	model base area, $\pi D^2/4$
U	=	time-average freestream velocity
α	=	angle of attack
δ_N	=	tip half-apex angle
θ	=	azimuth angle around circular cross section measured from the most leeward position
ν	=	kinematic viscosity of fluid
ρ	=	density of fluid
ϕ	=	roll angle

Introduction

THE experiments reported in the present Note and a related Note[1] are the extension of earlier work,[2] which experimentally studies the effects of freestream turbulence on the side force acting on an ogive cylinder at high incidence. In Ref. 2, the results indicate that freestream turbulence has different effects on flow past the ogive cylinder set at different roll angles. This is probably caused by different (nonuniform) microsurface imperfections on the body. Another factor that could play an important role is the state of the boundary layer. An earlier study[3] has shown that a boundary layer that is at/near a state of transition, that is, near the critical Reynolds number, is more responsive to freestream turbulence and undergoes an early transition to become a turbulent boundary layer. This has been known to cause a reduction in the aerodynamic loading on the body.

In Ref. 2, because of the speed (and, hence, Reynolds number) limitation of the wind tunnel used, the boundary layer of the ogive cylinder in the experiment was not near the transition state and the freestream turbulence did not cause the boundary layer to go through an early transition. To work around the described limitation and bring the boundary layer to the desired transition state, the authors

Received 24 February 2002; revision received 30 April 2002; accepted for publication 1 May 2002.

*Associate Professor, Department of Mechanical Engineering, 10 Kent Ridge Crescent.

†Research Fellow, Department of Mechanical Engineering, 10 Kent Ridge Crescent.

‡Senior Member of Technical Staff, Aeronautic Systems Programme, 20 Science Park Drive.